Modelling of Columnar-to-Equiaxed and Equiaxed-to-Columnar Transitions in Ingots Using a Multiphase Model

Nicolas Leriche, Hervé Combeau, Charles-André Gandin, Miha Zaloznik

Modelling of Columnar-to-Equiaxed and Equiaxed-to-Columnar Transitions in Ingots Using a Multiphase Model

N Leriche[1], H Combeau[1], Ch-A Gandin[2] and M Založnik[1]

[1] Université de Lorraine – Institut Jean Lamour, UMR CNRS 7198, 54011 Nancy, France
[2] Mines ParisTech – CEMEF, UMR CNRS 7635, 06904 Sophia Antipolis, France

E-mail: herve.combeau@univ-lorraine.fr

Abstract. We present a new method to handle a representative elementary volume (REV) with a mixture of columnar and equiaxed grains in ingot castings in the framework of an Eulerian volume averaged model. The multiscale model is based on a previously established fully equiaxed model. It consists of a three-phase (extra-granular liquid, intra-granular liquid and solid) grain-growth stage coupled with a two-phase (solid and liquid) macroscopic transport stage accounting for grain and nuclei movement.
In this context, we take into account the formation of a columnar structure and its development using a simplified front-tracking method. Columnar solidification is coupled with the growth of equiaxed grains ahead of the columnar front. The particularity of the model is the treatment of concurrent growth of mixed columnar and equiaxed structures only in the volumes that contain the columnar front. Everywhere else, the structure is considered either fully columnar or fully equiaxed. This feature allows for reasonable computational times even in industrial size castings, while describing the solutal and mechanical blocking phenomena responsible for the Columnar-to-Equiaxed Transition.
After a validation of the model, we discuss the numerical results for a 6.2-ton industrial steel ingot by comparison with experimental measurements. Final maps for macrosegregation and grain structures size and morphology are analysed. Furthermore, we quantify the impact of nuclei formation through fragmentation along the columnar front on the result.
An attempt at predicting the occurrence of the Equiaxed-to-Columnar Transition in the later phases of the process is also made.

1. Introduction

The following work is based on a multiphase volume-averaged model developed by Combeau and Založnik, which makes use of a numerical splitting technique [1,2]. Several studies of this research group about industrial ingots have already been presented concerning macro-segregation and grain morphology [3-5]. However, the columnar and equiaxed structures were only distinguished by defining a zone close to the mold where the grains were set to be fixed.

Efforts have recently been made to predict, thanks to multiphase models, the competition in industrial ingots between a columnar structure growing from the mold and transported equiaxed grains [6,7]. This multiphase model has been able to reproduce qualitatively the centerline macro-segregation in a 2.45-ton steel ingot. However, no comparison with CET observation was undertaken and the description of the equiaxed grain morphology remained simplified.

In the work presented thereafter, a complete model has been developed, including the growth of the columnar structures from the mold, their interaction with the equiaxed grains and especially the Columnar-to-Equiaxed-Transition (CET). The columnar grains can also grow from a packed equiaxed zone which leads to an Equiaxed-to-Columnar Transition (ECT).

The origin of the equiaxed grains in a steel ingot can be attributed to various causes including the detachment of grains formed in contact with the mold during filling or fragmentation of existing dendrites. This is the reason why different mechanisms for the formation of equiaxed grains have been investigated in the present model.

2. Description of the model

The present model is based on the fully coupled equiaxed model developed by Combeau and coworkers [1,2]. This model has been recently extended to take into account the presence of an inter-granular liquid [8] within the grain envelopes following the ideas of Rappaz and Thevoz [9]. Thus, the grain structure can be schematized as in Figure 1 where it was chosen to use a square envelope shape (ocathedral in 3D).

In this framework, the goal of this model is to take into account the apparition of columnar structures and their growth concurrently with the development of moving equiaxed grains. Based on previous models in the literature [10,11,12] we chose to use the same envelope shape and morphological parameters to model the columnar and equiaxed structures. In Figure 2, each columnar trunk is schematized by a regular assembly of sub-structures with a square envelope, arranged on a cubic lattice with characteristic length λ_1. The length $\ell(t)$ gives access to the propagation of the columnar front in the volume.

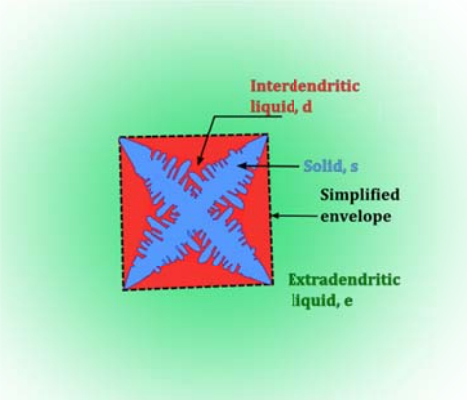

Figure 1. Schematic representation of a grain and its envelope together with the different phases.

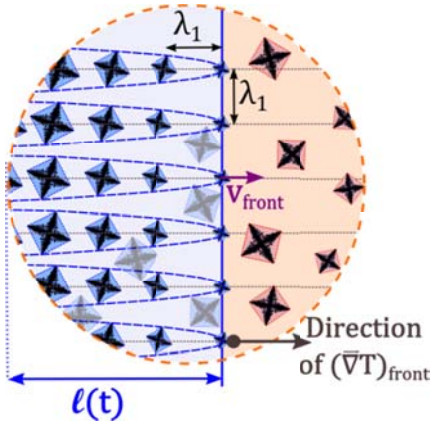

Figure 2. Schematic of a mixed volume containing both (blue, left) columnar and (red, right) equiaxed grains.

The main difference between the two types of structures lies in their origins. The columnar sub-structures are propagated by a front which initially originates at the mold and is connected to it, while the equiaxed grains take their origin in the dendrite fragments or nuclei. The position of the columnar front needs thus to be tracked during solidification. To this end, we make use of a method similar to the one developed by Ludwig and Wu [13]. Therefore, each representative volume can be located (i) behind the columnar front, (ii) contain the growing front or (iii) only contain liquid plus possibly equiaxed grains. In order to propagate the front further to neighboring volumes, a maximal length ℓ_{ref} of the front is defined in each averaging volume, similarly to the procedure in ref[13]. We considered that the direction of propagation of the columnar trunks is aligned with the local thermal gradient in the liquid ahead of the front $\left(\vec{\nabla}T\right)_{front}$. Consequently, ℓ_{ref} is simply the length of the

volume along the direction of $\left(\vec{\nabla}T\right)_{front}$. The velocity v_{tip} of the front at the columnar tips as well as the growth velocities of both the equiaxed envelopes and the columnar "sub-envelopes" are all calculated according to the LGK model [14].

In our model, a mixed volume containing both columnar and equiaxed structures as the one in Figure 2 is made of six phases. Three phases are associated with the equiaxed grains: the volume fraction of the solid phase g_s^{eqx} as well as the inter- and extra-granular liquid fractions g_d^{eqx} and g_e^{eqx} respectively. Similarly, we can define the variables g_s^{col}, g_d^{col} and g_e^{col} for the columnar structures such that: $g_s^{eqx} + g_d^{eqx} + g_e^{eqx} + g_s^{col} + g_d^{col} + g_e^{col} = 1$. In order to simplify the calculations, we suppose that the equiaxed grains present in a mixed volume containing the columnar front are fixed and only the liquid phase is allowed to move in these volumes. This approximation is only made for a layer of mixed volumes. The movement of equiaxed grains is accounted for ahead of the columnar front where columnar grains are not present. In the volumes containing only equiaxed structures, two flow regimes are considered. Where the local grains fraction g_{grain}^{eqx} is larger than the packing limit g_{env}^{pack}, the solid phase is fixed. The flow of the intragranular liquid is then described by a momentum equation for porous media including a Darcy term for the drag interactions. The permeability of the porous solid is modeled by the Kozeny-Carman law. For local grains fractions smaller than the packing limit $g_{gain}^{eqx} < g_{env}^{pack}$, the solid phase is considered to be in the form of free-floating equiaxed grains.

In accordance to most volume-averaged models of the literature, two phenomena responsible for the Columnar-to-Equiaxed Transition (CET) are considered:

1) Solutal blocking of the front. Its description is intrinsic to our model. Indeed, when the equiaxed grains grow, they enrich the equiaxed extra-granular liquid and thus reduce the chemical undercooling used to calculate v_{tip}. This liquid medium becomes solutally well-mixed, in which case v_{tip} is negligible and the columnar tips are effectively blocked.

2) "Mechanical" blocking. It occurs when the equiaxed grain fraction g_{grain}^{eqx} in a mixed volume containing the front reaches a critical value g_{lim}. This parameter has been used in previous studies with values ranging from 0.2 [15] to 1 [16]. In the present work, we used $g_{lim} = 0.5$ according to the geometric criterion proposed by Hunt [17].

At the top of industrial steel ingots, it is common to observe an oriented dendritic structure [3]. It is believed that this structure originates from a packed equiaxed zone when the sources of nuclei and fragments have been depleted [4]. As a consequence, this phenomenon can be assimilated to the restart of a columnar structure during what we call here the Equiaxed-to-Columnar Transition (ECT). Previously, it was necessary to artificially "renucleate" new equiaxed grains to be able to solidify the top of the ingots even with a non-uniform nucleation law [1]. We propose here a more physical way to deal with these zones according to the ECT idea: when the remaining liquid in front of an equiaxed packed zone is emptied of grains and nuclei, a new columnar structure is initiated in the volumes directly adjacent to the packed zone. These columnar trunks will interact with further remaining equiaxed grains and this will possibly lead to a subsequent CET.

The sources of these equiaxed grains have already be mentioned. However, most of the models applied to industrial ingots use either a three-parameter model [13] or a simple uniform model [1] to simulate the volumic heterogeneous nucleation of $n_0[grains.m^{-3}]$ equiaxed grains at undercooling $\Delta T_n[K]$. Yet, it remains unclear if there are a significant number of nucleation sites in non-inoculated alloys [18]. Another potentially important source of grains is through fragmentation of the columnar dendrites, especially in industrial ingots [19]. That is why the goal of this work is also to study the effect of a surface injection model at the columnar front. During the growth of the front, we consider a constant surface flux of equiaxed grains φ_0 $[grains.m^{-2}s^{-1}]$ which will be added to the adjacent liquid volumes that do not contain columnar structures. Because the initial sizes of the fragments are unknown, they will all be fixed to 1 μm, i.e. the same value as for the grains formed by heterogeneous nucleation. The only condition for the surface injection is that the quantity of solid in the mushy columnar zone is greater than the solid formed by the grains being injected.

When modeling the volumic heterogeneous nucleation of the grains, we account for the movement of the nuclei and suppose that they move at the same velocity as the liquid.

3. Case definition and experimental parameters

The present study concerns a 6.2-ton steel ingot cast by Ascometal Industries [3]. The experimental ingot has a square cross-section and a slightly conical shape. In the framework of our model, we consider a simplified 2D axisymmetric geometry of equal mass which is shown in Figure 3. Details concerning the thermal boundary conditions, the thermo-physical properties as well as experimental measurement of the morphologies and macrosegregation can be found elsewhere [3-5].

The ingot exhibits along the mold a roughly uniform columnar zone, between 7 and 11 cm thick. The ingot was cast with a hot-top consisting of a 3 cm thick insulating material. Shortly after the beginning of solidification, an exothermic powder is released besides the hot-top and produces heat by a chemical reaction which lasts for 5 minutes. This exothermic reaction causes significant remelting in the hot-top region and is believed to promote the breakdown of the columnar structure by fragmentation. Therefore, we could expect a thinner columnar zone in the hot-top and probably very few columnar structures originating from an ECT scenario.

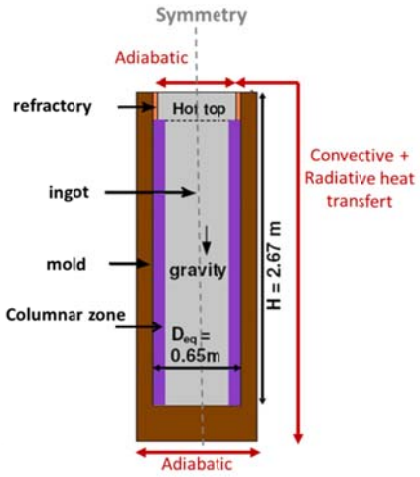

Figure 3. Geometry and boundary conditions for the 6.2-ton steel ingot.

Concerning the new parameter of the model, λ_1, a value of 1mm was chosen which corresponds to the average measured primary dendritic spacing in the columnar zone. It is noteworthy that the value of g_{lim} had only a very limited impact on the results in our case. The other parameters of the model are reported in a previous study on the same ingot [5]. Most notably the packing fraction for equiaxed grains was $g_{env}^{pack} = 0.4$, the alloy was simplified as a binary Fe-1.01 wt.%C and no pouring superheat was considered; i.e. the initial temperature of the liquid steel, T_0, is equal to the liquidus temperature $T_{liq}^0 = 1475\ °C$. The initial mold temperature is set to $25\ °C$.

The numerical domain was discretized into approximately 8600 cells for an average cell size of 1 cm. The time step is variable from $10^{-3}\ s$ to $0.1\ s$. The code is not parallelized and was run on a single Intel Xeon X5550 2.66 Ghz processor. The clock time for a typical simulation is about 60 hours.

4. Results and discussion

Results for volumic injections of equiaxed grains are showed in Figure 4. No fragmentation (surface injection at the columnar front) is considered and only a single class of nuclei n_0 in the range $[10^5; 10^9]$ $[nucl.m^{-3}]$ is activated at the liquidus temperature, i.e. with $\Delta T_N \approx 0\ K$. For comparison and to highlight the role of grains motion, simulation are carried out (wo) without and (w) with movement of the equiaxed grains. The black thick lines indicate the CET whereas the dashed zones bordered by thick white lines indicate columnar zones which have formed following an ECT event. The colour map indicates the equiaxed grain fraction g_{grain}^{eqx} in the whole ingot, characterizing notably the extent of the mixed columnar/equiaxed zones.

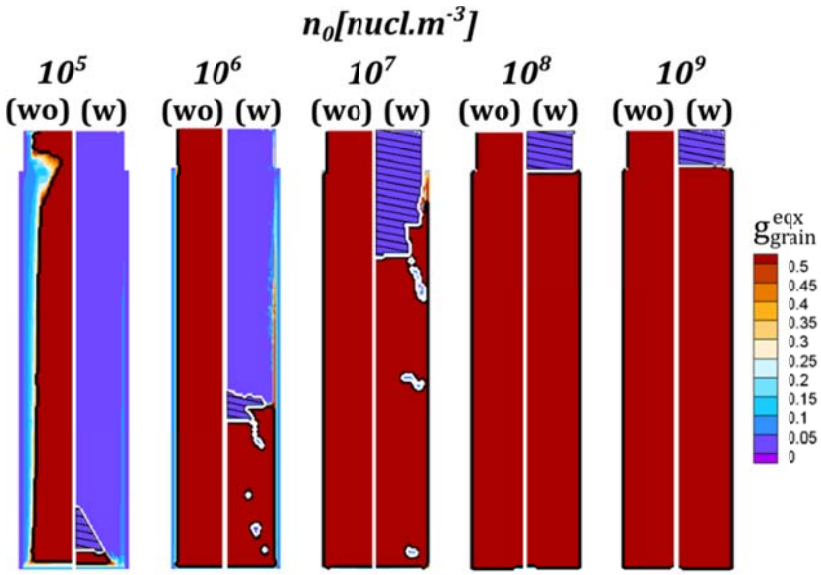

Figure 4. Predicted maps of the final equiaxed grain fraction g_{grain}^{eqx} as well as (thick black lines) the CET for increasing nuclei densities from 10^5 to 10^9 $[nucl.m^{-3}]$. We have assumed no nucleation undercooling. The columnar zones predicted following the ECT are shown as hatched zones bordered by white lines. For each case, the (wo) left map corresponds to fixed solid phases and the (w) right map to moving equiaxed grains.

Without accounting for grain motion and for values of n_0 greater than 10^7 $grains.m^{-3}$, the columnar zone is negligible and the ingot is predicted to have a fully equiaxed structure. This is shown in Figure 4 with $g_{grain}^{eqx} > 0{,}5$. For lower grain densities, we notice a roughly uniform columnar zone, except at the top of the ingot. For $n_0 = 10^5$ $grains.m^{-3}$, sweeping of colder yet not significantly enriched liquid at the bottom of the ingot near the beginning of solidification favours the growth of equiaxed grains. This explains why the front is blocked at the bottom first, leading to a thinner columnar zone. The columnar front is then blocked upwards in the ingot. In the hot-top region, complex thermal conditions and the interaction with the advancing front set up an enriched, cold liquid which is trapped in a clockwise convection cell. At the junction between the hot-top and the mold, this first liquid meets the relatively poorer and hotter liquid from the core of the ingot. Consequently, higher thermal gradients arise at this junction and favour the columnar structure which explains the wedge-like shape of the front there. Considering that without solid movement a computational volume cannot be emptied of equiaxed grains or nuclei, no ECT event is predicted in these cases. The macrosegregation profiles assuming a fixed solid are similar to previous results [5]. An example is shown in Figure 5. Here the average composition, $\bar{C}$, is normalized with the nominal composition C_0. The dashed curve represents the axial central segregation profile for $n_0 = 10^8$ $grains.m^{-3}$ without solid movement. Except for a negative segregation

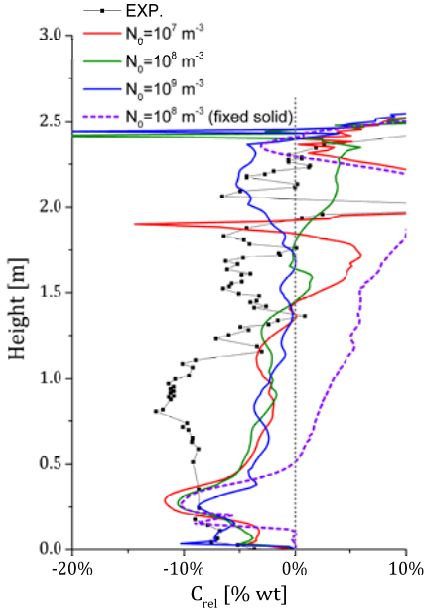

Figure 5. Comparison of the axial central segregation with measurements, where $C_{rel} = 100 \times \frac{(\bar{C}-C_0)}{C_0}$ [%].

at the bottom of the ingot and an inversion at the top, a strong positive segregation is predicted which is not in agreement with the experimental results. For other values of n_0, the results without solid movement are qualitatively similar. Especially, the position and height of the main positive segregation are the same, even though the intensity of this segregation can differ.

When taking into account the movement of the equiaxed grains, we notice a very dissimilar repartition of the structures in Figure 4. Starting from $n_0 = 10^6 grains.m^{-3}$, we see a clear distinction between a lower zone where the columnar thickness is very thin and an upper part which is entirely columnar. As n_0 increases, the equiaxed zone becomes larger and its boundary with the columnar zone moves upward. The top of the ingot always remains columnar. This can be explained by the fact that the motion of the equiaxed grains is controlled primarily by sedimentation. The grains first appear in the vicinity of the columnar front where the undercooling is maximal. Then, the grains grow rapidly and slide down along this region, thus participating to the formation a packed layer at the bottom of the ingot. Because of liquid convection, the whole ingot quickly becomes undercooled (except the top part) and the majority of the nuclei are activated. The newly formed grains directly fall at the bottom of the ingot and favour the growth of the packed layer. The local packing times (the times it takes for the grain in the equiaxed zone to become locally packed) are short and the sedimentation ends at $t \approx 300\ s$ in all cases. This value is to be compared with the total solidification time for the ingot, $t \approx 9000\ s$.After that, virtually no equiaxed grains remain in the liquid as evidenced by the negligible values of g_{grain}^{eqx} in the upper part of the ingot. Once the equiaxed grains have packed and nearly all the nuclei are activated, the columnar structure is free to develop in the remaining liquid. Remarkably, an ECT takes place at the top of the packed layer. The columnar structures originating from this ECT subsequently meet those growing from the mold. This is seen in Figure 4 with $n_0 = 10^6\ [nucl.m^{-3}]$ where a dashed blue region and a plain blue region are connected. The segregation profiles along the axis are shown in Figure 5 for three different densities of nuclei. The results are similar to previous calculations [5]. The best fit of the experimental results is found for $n_0 = 10^9\ nucl.m^{-3}$ but fails predicting the CET and is still not satisfying when considering the measured segregation profile.

The results presented in Figure 5 remain qualitatively valid when considering different nucleation undercoolings ΔT_N. A three parameter heterogeneous nucleation model [20], based on a Gaussian distribution, has also been tried. Comparable results were obtained, albeit with a more cone-shaped equiaxed zone.

It can be concluded that a volumic injection of nuclei fails to predict the observations. The volumic source of nuclei can be connected with heterogeneous nucleation or grains formed at the mold surface during the filling stage and then detached. It is already known that the fragmentation of dendritic columnar structures is another important source of equiaxed grains in industrial castings [19]. Thus, we investigate the influence of fragmentation on the results. The surface injection model mentioned earlier is now used for different flux values $\varphi_0\ [grains.m^{-2}s^{-1}]$ at the columnar front. The results are summarized in Figure 6 where no volume densities of nuclei were considered for these calculations. All calculations include grain movement as simulations with fixed solid do not produce realistic results. This stems from the fact that the fragments appear only in the liquid besides the front and need to be carried by the liquid to fill the centre of the domain. It is first noticeable that for $\varphi_0 = 10^2 grains.m^{-2}.s^{-1}$, the equiaxed zone has a much more pronounced cone shape than in previous volumic injection scenario.

The fraction of equiaxed grains entrapped in the columnar structures is also not negligible and the predicted structure can become considerably mixed especially at the top of the ingot, where remelting takes place. When the fragmentation flux is increased, a thin columnar zone is predicted in the lower part of the ingot whereas there is still a thick columnar zone in the upper part of the ingot. Nevertheless, the columnar zone at the bottom is not negligible with a CET at about 5 cm from the mold providing that $\varphi_0 \geq 4.10^2 grains.m^{-2}.s^{-1}$. The upper part is not entirely columnar in contrast with the case with the volumic density of nuclei scenario and the front is blocked at mid-radius. The

columnar zone directly besides the hot-top is thinner because of the thermal conditions and the fact that the columnar structures can re-melt due to the re-heating induced by the exothermic material present in the hot-top [3].

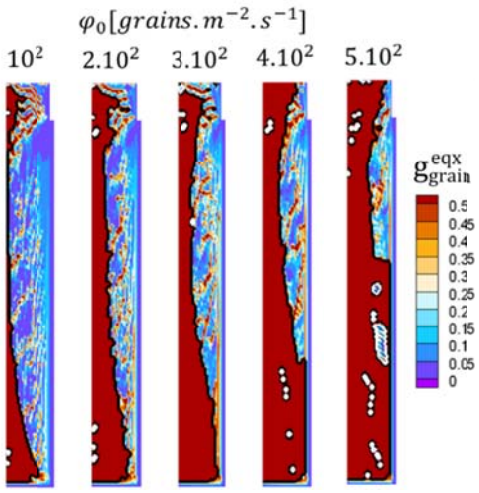

Figure 6. Predicted final equiaxed grain fraction g_{grain}^{eqx} as well as the CET and ECT for increasing fragmentation fluxes at the columnar front.

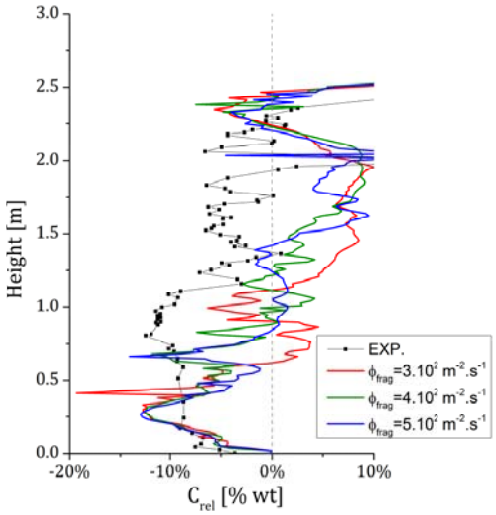

Figure 7. Comparison of the axial central segregation with the measurements where $C_{rel} = 100 \times \frac{(\bar{C}-C_0)}{C_0}$ [%]and for different fluxes.

The CET predicted which fits better the experiment can be explained in terms of packing behaviour of the equiaxed grains. As soon as the columnar structures appear at the mold, fragmentation takes place, producing new equiaxed grains which will at first instantly sediment along the columnar front. These first grains will not only contribute to the growth of a flat packed zone at the bottom, but also to the quick build-up of a vertical packed zone next to the front whose height is exactly that of the thin columnar region. This build-up takes place in about 200 s and causes the CET. The remaining fragments as well as the new ones coming from the front in the upper regions will then fill the rest of the ingot with a normal succession of horizontal layers. The whole ingot is filled with equiaxed grains in about 1300 s explaining why the columnar zone is thicker in the upper parts (except near the hot-top). As evidenced in Figure 6, there are few columnar structures originating from an ECT event contrary to the previous nuclei density model. Only dispersed spots of columnar zones can be seen in the core of the ingot.

The macrosegregation profiles at the centreline are reported in Figure 7 for the three highest fluxes. As we can see, the results at the bottom of the ingot are comparable to the calculations with the volumic nucleation model. In the top half of the ingot the results deviate from the experiment and a positive segregation is found. This corresponds roughly to the position where the columnar zone is too thick.

5. Summary and conclusions

Modelling of the columnar structure in ingot casting, its interaction with moving grains and the resulting CET and ECT have been implemented in a formerly purely equiaxed model [2].

Simulations were carried out for a 6.2-ton industrial steel ingot cast by Ascometal Industries. Two different origins of the equiaxed grains were studied: either a classical heterogeneous nucleation model or the injection of fragments in the liquid ahead of the columnar front. A parametric study for the nucleation densities suggests that this mechanism cannot accurately predict the experimental CET

in steel ingots because the source of grain in the liquid are eventually exhausted and the top of the ingot exhibit a purely columnar structure. The use of a fragmentation mechanism seems to give better results for the structures repartition most notably at the top of the ingot.

Both type of injection scenario give comparable results for the axial segregation. For example, using $\varphi_0 = 5.10^2 grains.m^{-2}.s^{-1}$ yields final equiaxed densities in the central part between $n_{eqx} = 10^6$ and $n_{eqx} = 10^7 grains.m^{-3}$. We can see on Figures 5 and 7 that calculations for $\varphi_0 = 5.10^2 grains.m^{-2}.s^{-1}$ and $n_0 = 10^7 grains.m^{-3}$ indeed show similar profiles for the axial segregation. The main difference is noticeable in the top third of the ingot, where the predicted structures are very dissimilar.

It has been reported in the literature [21] that during the filling stage of the ingot, numerous grains grow at the contact of the mold, then become detached and survive in the liquid as fragments or inoculants for the heterogeneous nucleation law. This points to the fact that both mechanisms could operate at the same time. However, our calculations with both nucleation and fragmentation do not exhibit significantly better results at the moment. We can therefore conclude that more work needs to be done to better understand the relative importance of these two mechanisms.

References

[1] Combeau H, Založnik M, Hans S and Richy P E 2009 *Metall. Mater. Trans.* B **40** 289
[2] Založnik M and Combeau H 2010 *Comp. Mater. Sci.* **48** 1-10
[3] Kumar A, Demurger J, Wendenbaum J, Založnik M and Combeau H 2012 *International Conference on Ingot Casting,Rolling and Forging, Aachen, Germany*
[4] Combeau H, Kumar A, Založnik M, Poitrault I, Lacagne G, Gingell A, Mazet T, Lesoult G 2012 *International Conference on Ingot Casting,Rolling and Forging, Aachen, Germany*
[5] Kumar A, Založnik M, Combeau H 2010 *Int. J. Adv. Eng. Sci. Appl. Math.* **2(4)** 140-148
[6] Li J, Wu M, Ludwig A and Kharicha A 2014 *Int. J. Heat Mass Transfer* **72** 668
[7] Li J, Wu M, Ludwig A, Kharicha A and Schumacher P 2014 *Materials Science Forum* **790** 121
[8] Bedel M 2014 Doctoral Thesis, Université de Lorraine, Institut Jean Lamour, Nancy, France
[9] Rappaz M and Thévoz Ph. 1987 *Acta Metall.* **35** 1487-97
[10] Martorano M A, Beckermann C and Gandin Ch-A 2003 *Metall. Mater. Trans.* A **34** 1657
[11] Dagner J, Friedrich J and Müller G 2008 *Comp. Mater. Sci.* **43** 872
[12] Ciobanas A I and Fautrelle Y 2007 *Journal of physics* D*: Applied Physics* **40** 3733
[13] Ludwig A and Wu M 2005 *Mater. Sci. Eng.* A **413-414** 109-114
[14] Lipton J, Glicksman M E and Kurz W 1984 *Mater. Sci. Eng.* **65** 57-63
[15] Biscuola V B and Martorano M A 2008 *Metall. Mater. Trans.* A **39** 2885
[16] Mirihanage W U and Browne D J 2011 *Shape Casting: The 4th Int. Symp.held at the TMS 2011 Annual Meeting & Exhibition, San Diego, California, USA*
[17] Hunt J D 1984 *Mater. Sci. Eng.* **65** 75-83
[18] Morando R, Biloni H, Cole G S and Bolling G F 1970 *Metallurgical Transactions* **1** 1407
[19] Paradies C J, Smith R N and Glicksman M E 1997 *Metall. Mater. Trans.* A **28** 875
[20] Rappaz M 1989 *Inter. Mater. Rev.* **34** 93-123
[21] Chalmers B 1963 *Journal of the Australian Institute of Metal* **8** 255